Electronic Supplementary Information for

High-Corrosion-Resistance Mechanism of Graphitized Platelet-type Carbon Nanofibers under OER in Concentrated Alkaline Electrolyte

Yuki Sato[a], Naohito Yamada[a], Sho Kitano[b]*, Damian Kowalski[b, c], Yoshitaka Aoki[b], and Hiroki Habazaki[b]*

[a] Graduate School of Chemical Sciences and Engineering, Hokkaido University, Sapporo, Hokkaido 060-8628, Japan

[b] Division of Applied Chemistry, Faculty of Engineering, Hokkaido University, Sapporo, Hokkaido 060-8628, Japan

[c] Biological and Chemical Research Centre (CNBCh), Faculty of Chemistry, University of Warsaw, ul. Żwirki i Wigury 101, 02-089, Warsaw, Poland

Corresponding Authors

E-mail: skitano@eng.hokudai.ac.jp (S. Kitano), habazaki@eng.hokudai.ac.jp (H. Habazaki)

Experimental Procedures

Carbon materials

According to a procedure described elsewhere, the pCNFs were prepared by the liquid-phase carbonization in a porous anodic alumina (AAO) template [1]. AAO template was prepared by anodizing 99.99 % pure aluminum sheets (TOYO Aluminum, 10×10 cm^2, thickness of 0.1 mm) at 40 V in a 0.3 mol dm^{-3} oxalic acid aqueous solution at 20°C for 2 h. The size of the nanopores in the anodic alumina layer was controlled by subsequent pore widening treatment in a 5 wt% H$_3$PO$_4$ aqueous solution for 0.5 h at 30°C. Under these conditions, the thickness and pore size of the porous alumina template was controlled at approximately 16 μm and 50 nm, respectively [1]. Polyvinyl chloride powder (PVC, SHIN-ETSU CHEMICAL Co., Ltd., TK-2500) was used as a carbon precursor. The AAO template and PVC powders were mixed and heat-treated at 300°C for 0.5 h with a temperature ramp of 400 K h^{-1} in a stream of high-purity argon (99.999 %) followed by heat treatment at 600°C for 1 h. During this heat treatment, PVC was converted into a liquefied pitch-like intermediate at ~350°C [2-4], penetrating into the cylindrical pores of the AAO template. Then, during further heat treatment at 600°C, carbonization of the pitch-like intermediates proceeded [1-4]. After cooling, the template was dissolved in a 20 wt% NaOH aqueous solution under ultrasonication, and the pCNFs were filtered. Further heat treatment was performed at 2000 or 2400°C in a stream of high-purity argon (99.999 %) using the high-temperature furnace (Kurata-Giken, KVA-40/50) and a graphite crucible. Depending on the heat treatment temperature, pCNFs were denoted, for instance, as pCNF2000 and pCNF2400. The temperature of 2400°C was the highest temperature of the available furnace. To examine pCNFs with a higher graphitization degree, the commercial pCNF3000 (Carbon Nanochips, Sigma-Aldrich) [3], which was heat-treated at 3000°C, was also used in this study. In addition, to compare pCNFs with other nanostructured carbon materials, two-types commercial carbon materials, *i.e.,* Toka Black (TB, TOKAI CARBON, #3800) and acetylene black (AB, STREM Chemicals, 100% compressed), were also used. These carbon materials were chosen because of their easy processability and availability.

Characterizations

The phase purities and the graphitization degrees of the carbon materials used in this study were examined by X-ray powder diffraction (XRD, Rigaku, Ultima IV) using Cu Kα radiation ($\lambda = 0.15418$ nm, $U = 40$ kV, $I = 20$ mA). The graphitization degree was also examined by Raman spectroscopy (Horiba Scientific, XploRA) using a 532 nm laser beam with an incident power on the sample of 2.5 mW. The spectral range investigated using a 2400 lines mm^{-1} grating was from 800 to 2000 cm^{-1}. Nitrogen gas adsorption/desorption isotherm measurements (Bel Japan, Belsorp-mini instrument) were conducted at $-196°C$ to estimate the BET surface areas. Prior to the adsorption measurements, samples were degassed at 150°C for 20 h. The surface of specimens was observed using a field-emission scanning electron microscope (Zeiss, Sigma-500), operated at 1.5 kV, with an in-lens secondary electron detector. For scanning transmission electron microscopy (STEM) combined with electron energy-loss spectroscopy (EELS) and TEM imaging, an FEI Titan3 G2 60-300 was used with an acceleration voltage of 300 kV.

Identical-location observation study

In order to investigate the corrosion rate of each carbon material and the crystalline plane dependency of corrosion, the ILSEM technique was used [4]. The gold mesh grid (Alliance Biosystems, SlimBar Index Grids Gold, 2290G-XA), which was anodized at 2.4 V vs Ag/AgCl in a 0.3 mol dm^{-3} oxalic acid aqueous solution at 0°C for surface roughening [5, 6] (**Figure S2a**), was used as a substrate in this study. The anodizing curve and comparison of surface morphology before and after the anodizing were shown in **Figure S2**. After the anodizing, the grid was irradiated with oxygen plasma for 5 minutes using a Harrick Plasma PDC-32G air plasma cleaner to remove a contaminant hydrocarbon surface layer [7]. Then, the carbon materials were loaded on the gold grid by immersing it into the ethanol solution containing 10 mg mL^{-1} carbon and 5% Nafion. Finally, the carbon-loaded Au grid was dried in the incubator (Yamato, DKN302) at 250°C.The carbon-loaded grid was first observed by a low-acceleration voltage SEM. Then, the grid was anodically polarized at 1.8 V vs RHE in a 4.0 mol dm^{-3}

KOH aqueous electrolyte for selected periods at room temperature, followed by SEM observations to estimate the corrosion rate from the outer shape changes (**Figure S2d**). These anodized specimens were also served for STEM/EELS experiments. The electrochemical measurements were conducted using a potentiostat (Princeton Applied Research VersaSTAT3) controlled by the computer. Platinum foil and Hg/HgO/4 mol dm^{-3} KOH electrodes were used as counter and reference electrodes, respectively. The electrode potential was converted from the Hg/HgO/4 mol dm^{-3} KOH reference scale to the RHE using the following equation [1]:

$$U \text{ vs RHE} = U \text{ vs Hg/HgO/4 mol dm}^{-3} \text{ KOH} + 0.098 + 0.059 \times \text{pH} \qquad (1) [1]$$

Wettability measurements

The surface wettability of carbon materials was examined before and after anodic polarization at 1.8 V vs RHE in an Ar-saturated 4.0 mol dm^{-3} KOH electrolyte for 2 h. The carbon materials were loaded on a flat glassy carbon substrate (GC, Pine, AFED050P040GC, ϕ = 5 mm) using a carbon/Nafion mixed solution. The mixed solution was prepared by ultrasonically dispersing the carbon powders (10 mg) in a mixture of 0.2 mL of 5 wt% Na^{+}-exchanged Nafion solution and 4.8 mL of ethanol. The wettability of the carbon materials was evaluated by measuring the static water contact angle of Milli-Q water (1 μL) using an optical contact angle meter (Kyowa Interface Science, DM-CE1).
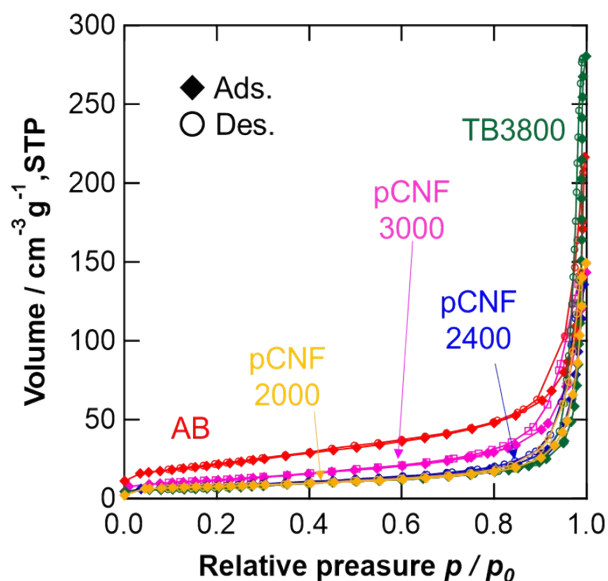
Supporting Figures and Tables

Figure S1. N_2 adsorption/desorption isotherms at -196°C of the carbon materials used in this study.
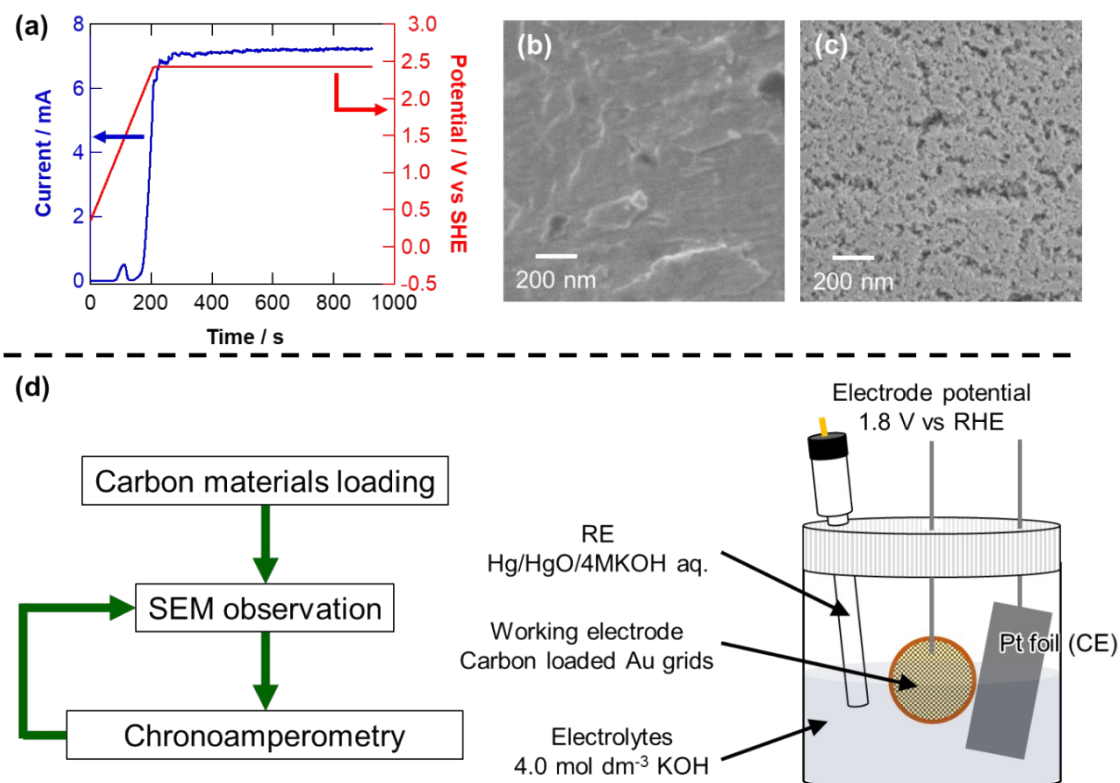

Figure S2. (a) Typical current-time and potential-time curves during the anodizing of an Au grid in 0.3 mol dm^{-3} oxalic acid solution, (b, c) Surface SEM images of Au grids (b) before and (c) after the anodizing shown as Fig. S1a. (d) The procedure and electrochemical cell of ILSEM study.
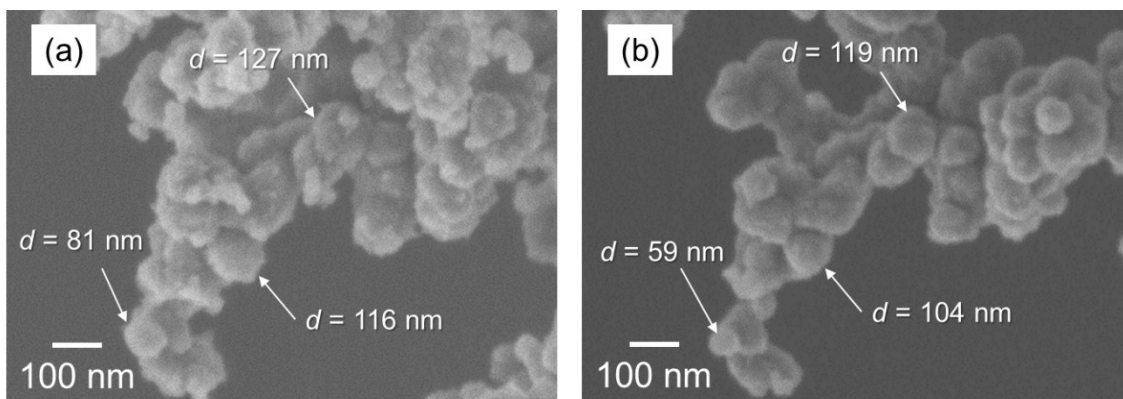
Figure S3. (a, b) Identical-location SEM observation images of AB loaded electrode (a) before and (b) after polarization at 1.8 V vs RHE for 24h.
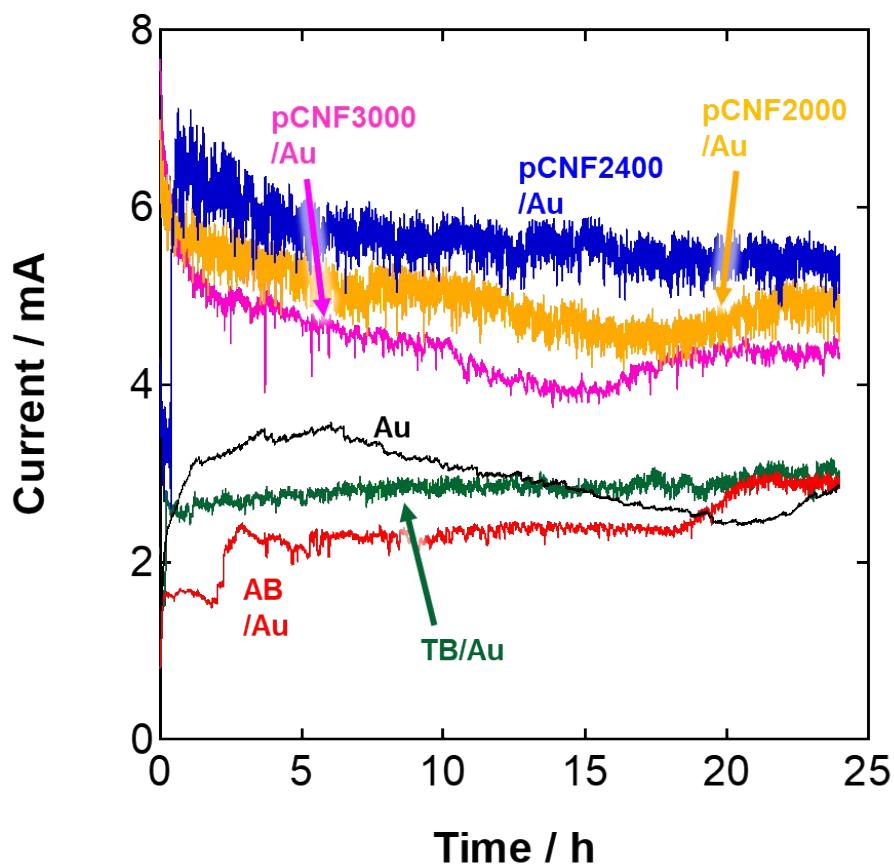
Figure S4. Current-time curves of identical-location experiments measured at 1.8 V vs RHE in 4.0 mol dm^{-3} KOH aq.
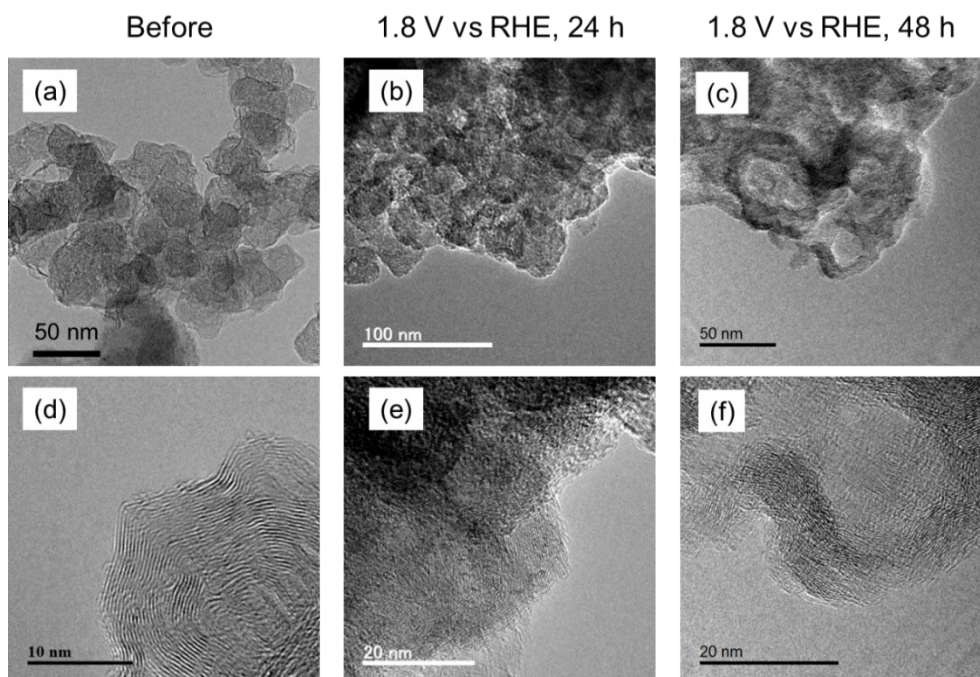
Figure S5. TEM images of AB (a, d) before and after the polarization at 1.8 V vs RHE in 4.0 mol dm^{-3} KOH aq. electrolyte for (b, e) 24 h and (c, f) 48 h.
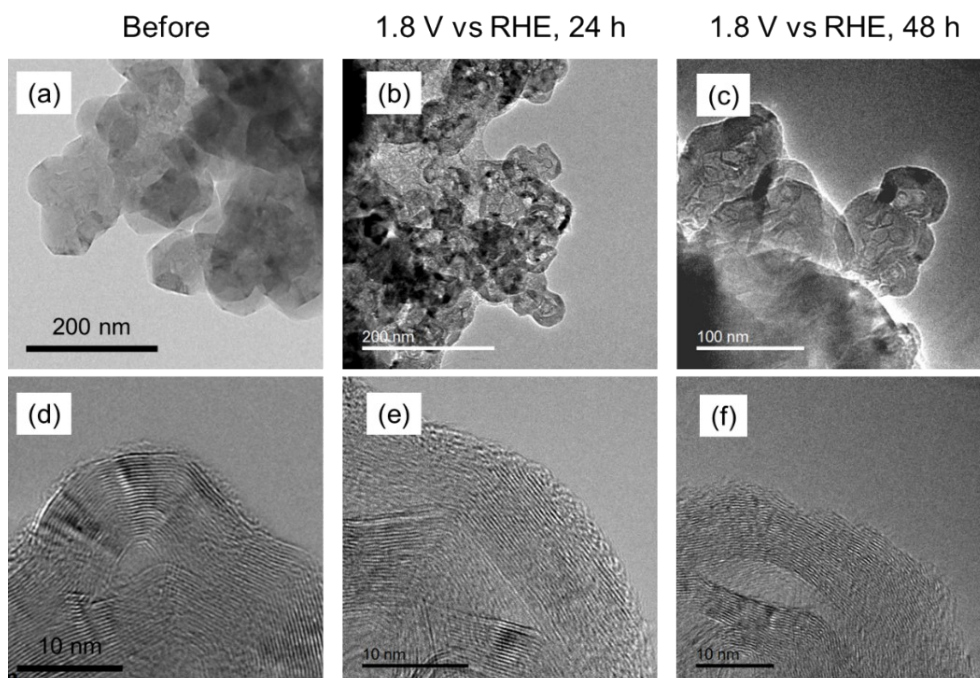

Figure S6. TEM images of TB (a, d) before and after the polarization at 1.8 V vs RHE in 4.0 mol dm^{-3} KOH aq. electrolyte for (b, e) 24 h and (c, f) 48 h.
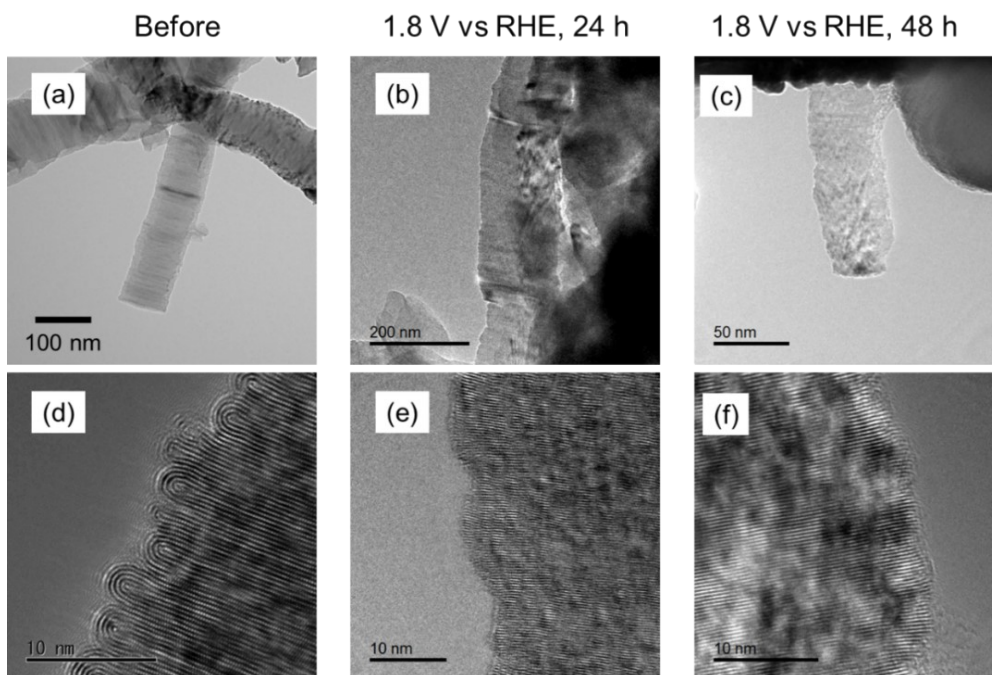
Figure S7. TEM images of pCNF2000 (a, d) before and after the polarization at 1.8 V vs RHE in 4.0 mol dm^{-3} KOH aq. electrolyte for (b, e) 24 h and (c, f) 48 h.
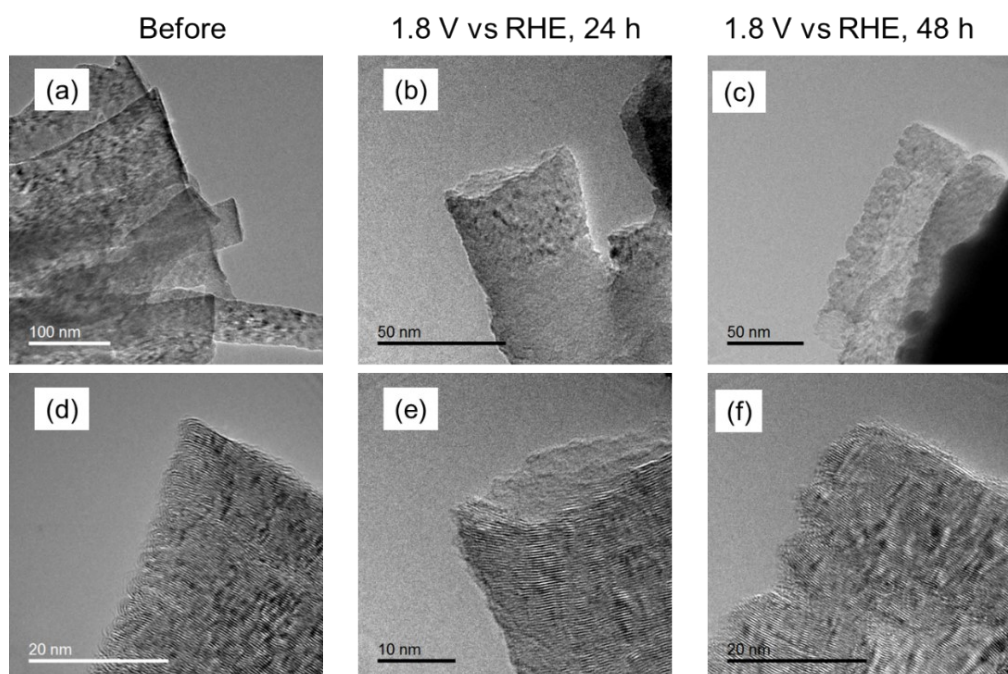

Figure S8. TEM images of pCNF3000 before and after the polarization at 1.8 V vs RHE in 4.0 mol dm^{-3} KOH aq. electrolyte for (b, e) 24 h and (c, f) 48 h.
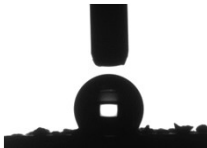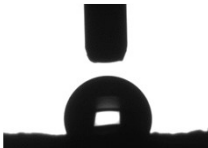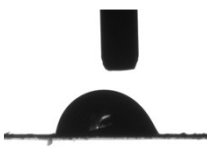
	TB / deg.	pCNF2400 / deg.
Before	115.7 $\pm$ 14.5	109.8 $\pm$ 2.3
1.8 V $_{vs RHE}$, 2h	79.6 $\pm$ 7.7	25.5 $\pm$ 8.0

Figure S9. Contact angles for the static Mili-Q water on the carbon electrodes before and after the anodic oxidation at 1.8 V vs RHE in 4.0 mol dm^{-3} KOH aq. electrolyte for 2 h. Each experiment was repeated five times.

Table S1. The lattice spacing values of each carbon material calculated from the XRD pattern.

	Lattice spacing, d_{002} estimated from the XRD pattern / nm	References
pCNF1000	0.348	[8]
pCNF1500	0.346	[8]
pCNF2000	0.343	This work
pCNF2400	0.340	This work
pCNF3000	0.336	This work
DB	0.346	[1]
DB2400	0.345	[1]
TB	0.342	This work
AB	0.352	This work
MW	0.339	[1]

Table S2. EELS peak list of functional groups of carbon materials [9-13].

Energy / eV	Functional group
285	Aromatic C-C
286.0 – 286.8	Ketone O=C
	Nitrile N≡C
	Phenol HO-C
286.6	Ether C-O-C
287.2–288.3	Aliphatic C–C
288.5 – 288.7	Carboxyl O=CO-
290.3	Carbonate CO_3^{2-}

References of Electronic Supplementary Information

[1] Y. Sato, D. Kowalski, Y. Aoki, H. Habazaki, *Appl. Cat. A: General*, **2020**, 597, 117555.

[2] R. Hurt, G. Krammer, G. Crawford, K. Jian, C. Rulison, *Chem. Mater.,* **2002,** 14(11), 4558-4565.

[3] D. Dollimore, G.R. Heal, *Carbon,* **1967,** 5, 65-72.

[4] Y. Bai, Z. Wang, C. Wu, R. Xu, F. Wu, Y. Liu, H. Li, Y. Li, J. Lu, K. Amine, *ACS Appl. Mater. Interfaces,* **2015,** 7(9), 5598–5604.

[3] S. George, H.K. Lee, *J. Phys. Chem. B*, **2009**, 113(47), 15445–15454.

[4] N. Hodnik, G. Dehm, K.J.J. Mayrhofer, *Acc. Chem. Res.*, **2016**, *49*, 2015−2022

[5] K. Nishio, H. Masuda, *Angew. Chem. Int. Ed.,* **2011**, 50(7), 1603-1607.

[6] K. Nishio, H. Masuda, *Bull. Chem. Soc. Jpn.*, **2013**, 86(10), 1144-1150.

[7] T. Inoue, A. Koyama, D. Kowalski, C. Zhu, Y. Aoki, H. Habazaki, *Phys. Status Solidi A,* **2020,** 217(13), 190836.

[8] H. Habazaki, M. Kiriu, M. Hayashi, H. Konno, *Materials Chemistry and Physics,* **2007,** 105, 367-372

[9] C. Vollmer, D. Kepaptsoglou, J. Leitner, H. Busemann, N.H. Spring, Q.M. Ramasse, P. Hoppe, L.R. Nittler, *PNAS,* **2014***, 111, 15338-15343.

[10] K. Miyazawa, T. Nagai, K. Kimoto, M. Yoshitake, Y. Tanaka, *Surf. Interface Anal.*, **2021**, 53(1), 84-89.

[11] K. Miyazawa, T. Nagai, K. Kimoto, M. Yoshitake, Y. Tanaka, *Surf. Interface Anal.*, **2020**, 52(1-2)*, 23-33.

[12] M. Pelaez-Fernandez, A. Bermejo, A.M. Benito, W.K. Maser, R. Arenal, *Carbon,* **2021,** 178(30), 477-487.

[13] A. Braun, F.E. Huggins, N. Shah, Y. Chen, S. Wirick, S.B. Mun, C. Jacobsen, G.P. Huffman, *Carbon,* **2005,** 43(1), 117-124.